

Adaptive enhancement based on a visual model

Eli Peli, MEMBER SPIE

Eye Research Institute
20 Staniford Street
Boston, Massachusetts 02114
and

Departments of Ophthalmology
New England Medical Center
Tufts University School of Medicine
Harvard Medical School
Boston, Massachusetts

Abstract. The human visual system is capable of detecting and following the course of striated periodic patterns, even under adverse conditions of poor contrast and low signal-to-noise ratio. Sections of a striated pattern of subthreshold contrast may be detected easily if other parts of the same pattern have suprathreshold contrast. To simulate these capabilities of the visual system, an image processing algorithm was developed using basic "cells" that are well localized in both the space and spatial frequency domains. These band-limiting, orientation-sensitive "fan filters" are similar in their point spread functions to the two-dimensional Gabor functions commonly used to describe responses of visual cortical cells. These filters are used both to detect the orientation of the striated pattern in a small window and to enhance the image in that orientation. The search for local orientation is limited to a small range based on orientations found in neighboring, overlapping windows. The orientation of the maximally responding cell is used for the enhancement. Results of applying the adaptive directional enhancement to nerve fiber layer photographs, fingerprints, and seismic data are presented.

Subject terms: visual communications; image processing; adaptive processing; directional enhancement; image enhancement; nerve fiber layer; receptive fields; visual model.

Optical Engineering 26(7), 655-660 (July 1987).

CONTENTS

1. Introduction
2. Methods
 - 2.1. Algorithm
 - 2.2. Filters
3. Results
4. Discussion
5. Acknowledgments
6. References

1. INTRODUCTION

Patterns of families of curved lines occur under many circumstances. Such striated patterns are seen in fingerprints, photographs of the retinal nerve fiber layer,¹ histologic preparations of the corneal stroma,² and seismic data.³ The human eye can follow the course of such patterns even when the image quality is poor. An image enhancement technique with similar capabilities could be valuable in the image analysis of such patterns. In this report the development of an adaptive orientation-sensitive enhancement algorithm for curved striated patterns based on a human visual model is described.

Subjectively, it appears that one's vision is "tuned" to the size and spacing of lines to enable better detection. It also seems that, to help visualize a degraded area, we use peripheral information from other portions of the image to predict

the most likely course or orientation of the pattern. Furthermore, if a low contrast, subthreshold portion of such an image is viewed together with contiguous suprathreshold portions of the same image, the pattern becomes clearly visible in the previously subthreshold area. Patients tested with the contrast sensitivity plate test (Arden test)⁴ frequently report this response. Once the suprathreshold portion of the plate is seen, the pattern is followed easily to the top of the plate "into regions which a moment before appeared a uniform gray."⁴

The algorithm presented here implements two-dimensional filters based on the mathematical description of responses recorded from visual cortical cells. Visual cortical neurons are associated with a receptive field; when illuminated, a retinal area will cause the cells to respond. If one assumes linearity, the cell's response to any stimulus can be characterized by its impulse response in the space domain or by its transfer function in the frequency domain. In area V_1 of the brain's visual cortex, many cells have similar characteristics and are called simple cells. These cells, receiving direct stimulation from the retina, are organized in an orderly manner such that cells with the same or close receptive fields are adjacent to one another in the brain. A recent description of the responses of simple visual cortical cells has used the Gabor functions⁵ to represent the receptive field impulse response and the corresponding spatial frequency transfer function. The Gabor functions, each of which is described as a sine function multiplied with a Gaussian envelope, reach the theoretical limit of joint information resolution for spatial frequency and spatial position.⁶ The transfer function of these cells is described in the frequency domain as an elliptical

Paper VC-113 received Oct. 2, 1986; revised manuscript received Jan. 30, 1987; accepted for publication Jan. 30, 1987; received by Managing Editor March 5, 1987. This work was presented at the annual meeting of the Association for Research in Vision and Ophthalmology, Sarasota, Fla., May 1986.

© 1987 Society of Photo-Optical Instrumentation Engineers.

two-dimensional Gaussian envelope. Each cell, thus, optimally responds to stimuli of specific spatial frequency at a specific orientation. The cell will respond less to stimuli in a range of orientations and frequencies within its bandwidth. The ratio of the bandwidth to center frequency is fairly constant since smaller receptive fields are associated with a higher spatial frequency response.

The Gabor functions are not separable in polar coordinates in either domain.⁷ However, despite the limited data available, there is a significant tendency for the measured simple cell transfer functions to align radially in the two-dimensional frequency plane.⁸ Cells with the same receptive fields and spatial frequency response are found in columns. The orientation to which each cell is most sensitive changes gradually along these columns. These hypercolumns,⁹ describing the set of neurons that span all orientations, also suggest a polar-coordinate organization in the frequency domain. For these reasons and for relative ease of calculation, the filters implemented in this study were fan filters,¹⁰ separable in polar coordinates in the spatial frequency domain. The general fan-filter transfer function is described as

$$F(u,v) \equiv F(q,\phi) = H(q)G(\phi), \quad (1)$$

where $H(q)$ and $G(\phi)$ represent the radial and angular profiles of the filter, respectively; q and ϕ are the polar coordinates; and u and v are the Cartesian coordinates in the spatial frequency domain.

In addition to the radial organization in the frequency domain, the receptive field's organization in the visual cortex also represents a radial arrangement in the spatial domain. The major axis of a receptive field tends to lie along a line connecting the receptive field to the area centralis.¹¹ To simulate this radial organization, a serial algorithm was developed that maintained radial organization using a progression on a growing spiral. The first receptive field to be processed was selected by the operator, and subsequent cells were selected on the growing spiral centered on this receptive field. This paradigm enabled the processing to progress from an area of the largest signal-to-noise ratio outward into areas of a smaller SNR.

2. METHODS

2.1. Algorithm

The algorithm is applied to one small subimage (window or receptive field) at a time. In the search phase the subimage is Fourier transformed (FT) to the frequency domain, and the orientation of the striations is detected by applying a series of fan filters at different orientations to the FT of the window and selecting the one with the maximal response. In the filtering phase, the output of a filter with the same orientation as the maximally responding filter is retransformed to the spatial domain. The image in the processed window is then averaged with the images obtained in overlapping windows.

The operator selects initial parameters such as window size, selected as $2^n \times 2^n$ pixels, and the amount of overlap of processing windows (0 to 50%). For the examples presented here, a window size of 64×64 pixels ($n = 6$) and an overlap of 50% were selected. The operator then selects the angular parameters of filters used in the search phase. Commonly, a fan width of 10° and a search every 5° are used. These parameters were selected by experimenting with various combinations on several nerve fiber layer images. The operator also

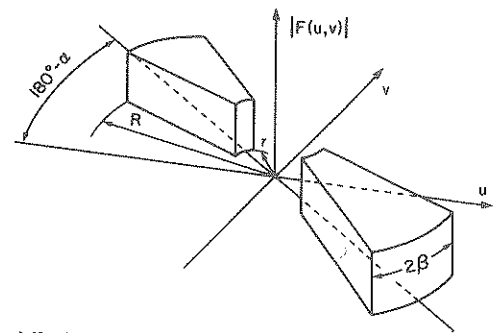


Fig. 1. Band-limited fan filter with rectangular profiles both radially and angularly. This filter serves as the first approximation of the cortical cells' response since it is band-limiting and directionally selective. This filter was implemented in the search phase of the algorithm.

defines the spatial frequency bandwidth of the search-and-enhancement filter by selecting the low and high cutoff frequencies. The specific algorithm applied to process an image was

- (1) Select the next local processing window.
- (2) Transform the image in the window to the spatial frequency domain via fast Fourier transform (FFT).
- (3) Display the power spectrum in place of the window.
- (4) From the eight neighboring windows, find those that have already been processed, and average the orientations selected for those windows.
- (5) Within a limited range around the average orientation, search for the orientation of the strongest responding fan filter.
- (6) Multiply the FT of the image with a filter centered at the orientation found in step 5.
- (7) Display the filtered spectrum.
- (8) Transform the filtered image back to the space domain via inverse FFT.
- (9) Average the image with overlapping windows.
- (10) Go to step 1.

The spectra in steps 3 and 7 of the algorithm are displayed only to enable the operator to observe the process; no interactive response is required.

2.2. Filters

To reduce calculation time, a simple filter was applied during the orientation search phase (steps 4 and 5). This filter, representing a first approximation of cortical cell responses, is a sharp bandpass filter in both angular direction and spatial frequency. Figure 1 illustrates the filter's transfer function, $F(u, v) = H(q)G(\phi)$. Here

$$H(q) = \begin{cases} 1 & r < q < R \\ 0 & \text{elsewhere,} \end{cases} \quad (2)$$

where $[r, R]$ represents the spatial frequency range of the filter, and

$$G(\phi) = B(\phi - \alpha) + B(\phi - \alpha - 180^\circ), \quad (3)$$

where

$$B(\phi) = \begin{cases} 1 & -\beta < \phi < +\beta \\ 0 & \text{elsewhere,} \end{cases} \quad (4)$$

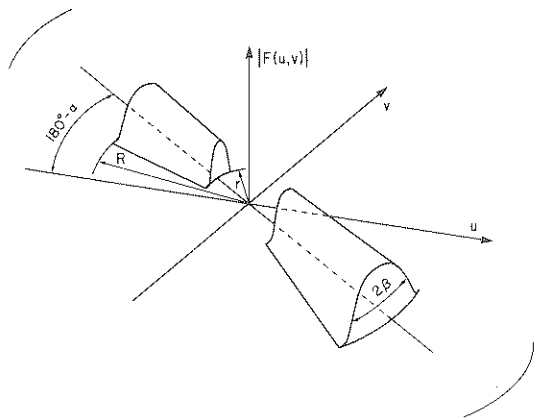


Fig. 2. Fan filter with a Gaussian angular profile was implemented as the second-order approximation of the cortical cells' response function and was used to enhance the striated patterns.

α is the filter orientation in the frequency domain, corresponding to orientation sensitivity at $90^\circ + \alpha$ in the space domain, and 2β is the angular bandwidth. The search was performed within a restricted angular range surrounding the local average orientation (step 5). Filters of angular widths of 10° with angular overlap of 5° (50%) were applied to the windows' two-dimensional FT. The orientation of the filter with the maximal normalized response was selected as the orientation of the striation in the window. The response was normalized to the number of points within the filter, which varied with the angle because of the discrete nature of the data. The filters were also band-limiting in the radial spatial frequency axis. A 1.5- to 2-octave width was selected by the operator to match the response of cortical cells.⁷ The speed of calculation was significantly increased by using look-up tables to assign the angle and radius of each point in the local processing window.

If a fan filter with a rectangular angular profile is applied to the image (step 6), a significant "ringing" is evident.¹ Therefore, the angular profile of the filter was smoothed by a Gaussian multiplier (Fig. 2):

$$B(\phi) = \frac{A}{\pi\beta} \exp\left(-\frac{\phi^2}{\beta^2/2}\right), \quad (5)$$

where A is an amplification factor.

The angular width of the filter used for the filtering phase was selected as 30° to match the reported directional sensitivity of the simple cortical cell¹² and the directional selectivity predicted by the Gabor functions for a 1.5-octave filter.⁷ The spatial frequency bandwidth was the same 1.5 to 2 octaves as used during the search phase. However, to maintain some of the low frequency details in the images for the applied filter, the spectrum outside this range was not eliminated completely:

$$H(q) = \begin{cases} 1 & r < q < R \\ 0.1 & 0 < q < r \\ 0 & R < q. \end{cases} \quad (6)$$

This facilitates localization in images with clear landmarks oriented differently from the enhanced striations. The response of simple cells does roll off at a low frequency but is not extinguished completely.

The calculations required for the Gaussian filter profile were also reduced by using look-up tables.

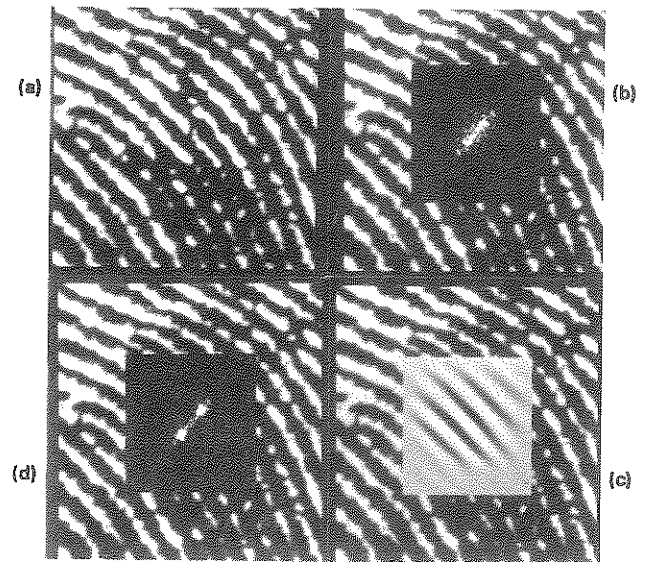


Fig. 3. Operation of the orientation-sensitive enhancement on one window (receptive field) of the fingerprint image. (a) Section of the original image with the local processing window highlighted. (b) Orientation of the striations is evident as a series of peaks in the orthogonal direction in the magnitude of the Fourier transform. (c) The transform after filtration with the directional filter centered around the automatically detected orientation. (d) The filtered image window after retransformation to the space domain.

3. RESULTS

The operation of the algorithm, using one 64×64 pixel window from a fingerprint image, is illustrated in Fig. 3. In the case of a fingerprint, the orientation of the striations can be noted easily from a series of peaks in the orthogonal direction in the power spectrum [Fig. 3(b)]. This orientation was automatically detected in the search phase, and a fan filter with a Gaussian profile in this orientation was used to amplify this part of the spectrum [Fig. 3(c)]. The filtered image was then retransformed to the spatial domain via the inverse FFT [Fig. 3(d)].

The effect of the process on a full fingerprint image is illustrated in Fig. 4. This is the same image used by Lehar and Gonsalves³ in their study of local adaptive enhancement. The results illustrated here are superior to the nondirectional enhancement previously applied to such images (both optical bandpass filters¹³ and digital nonlinear bandpass filters³) because noise along the striations is reduced significantly and small gaps are filled. Simultaneously, the so-called minutiae of the fingerprints, such as ridge endings and bifurcations, are maintained in the processed image.

The directional enhancement algorithm has difficulty processing such areas as nodes and deltas in the fingerprints. At a nodal area in the fingerprint the curvature of the striations is increased, and there are two orthogonal orientations. In the delta's neighborhood no single correct orientation exists; rather, three orientations coincide. Such data with no unique orientation may result in orientation search phase errors that can propagate further [see Fig. 4(b)]. These problems may be sensed automatically by calculating the variability in orientation of neighboring windows. If large variability is noted, the window can be processed without orientation sensitivity (i.e., just bandpass filtered), or the window size may be reduced to enable better detection of local orientation. Both approaches were applied to the image with satisfactory results (Fig. 5).

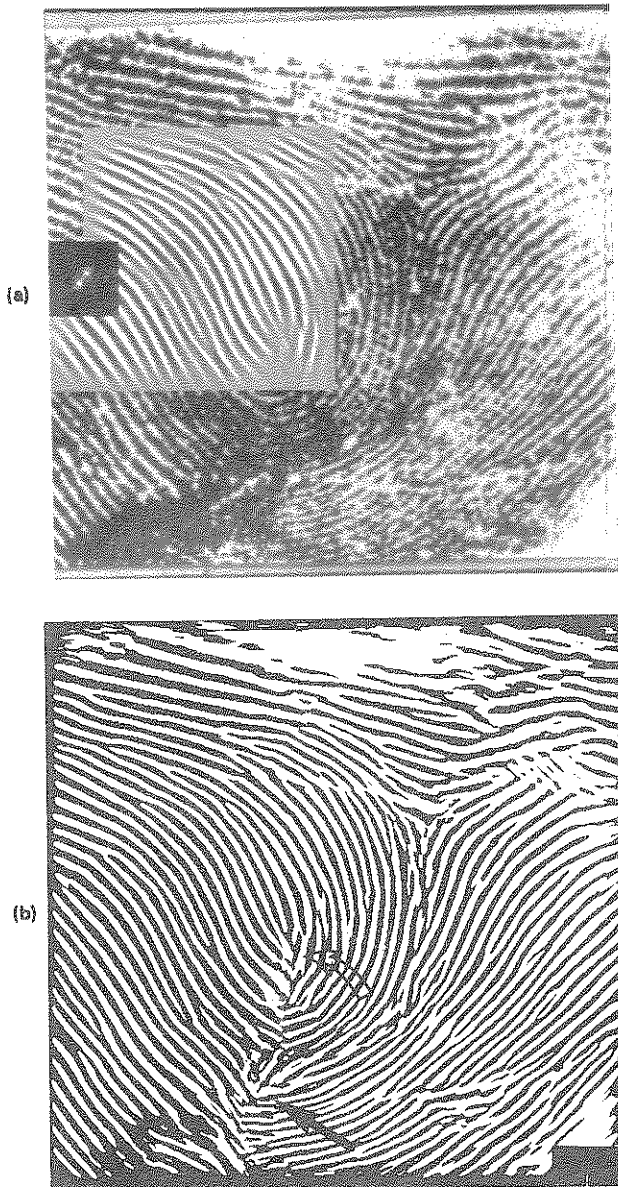


Fig. 4. Results of orientation-sensitive enhancement of fingerprint image. (a) Original image with a section already processed. (b) Fully processed image after binarization by thresholding at midlevel (128). Note errors in processing near the delta and node and propagation of the error near the node (arrows).

Orientational filtering with smaller window size was found to provide better results and may represent a better simulation of the visual system's approach since cortical cells of various receptive field sizes are available [Fig. 5(b)].

The result of applying the algorithm to images of the retinal nerve fiber layer is illustrated in Fig. 6. This fine striation pattern is low in contrast, yet the algorithm can detect and enhance both normal striations and the appearance of slit defects in the nerve fiber layer. Because the curvature of the nerve fiber pattern is small relative to the fingerprint image, a more limited search range can be used for this pattern (30° rather than the 60° used for the fingerprint image), which reduces the chance of errors. Adaptive enhancement followed by binarization may be useful in evaluating the normal nerve fiber layer and diffuse atrophy.

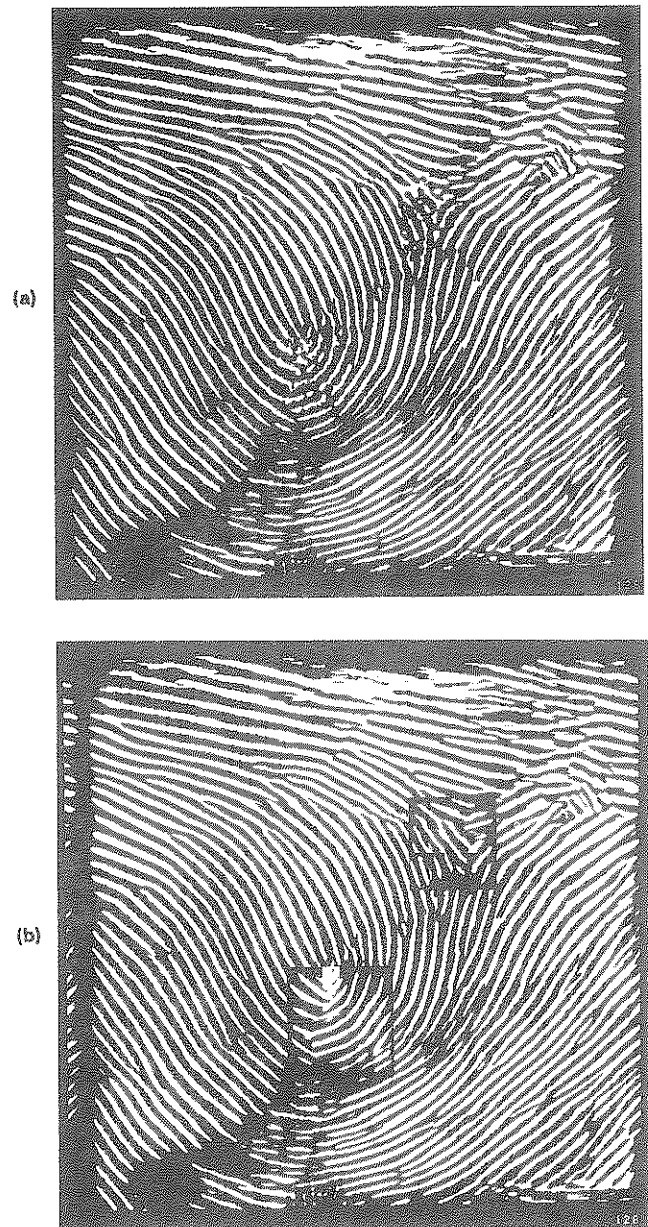


Fig. 5. Comparison of processing of difficult points in the image, such as nodes and deltas, with (a) nondirectional enhancement and (b) orientation-sensitive enhancement with reduced window size. Windows of 32×32 were used within areas around the node and delta. Note that elimination of the error at the node [(a) and (b)] prevents its further propagation.

Results of applying the algorithm to seismic data followed by thresholding binarization are illustrated in Fig. 7. This stacked seismic section represents a few miles across the image, and the striated pattern reflects the organization of the geologic layers. In the processed image the noise is significantly reduced, and the artifacts of vertical lines are completely eliminated. The important striation patterns of the geologic structures are maintained, as are the spatial phase relationships across shearing areas.

4. DISCUSSION

Incorporating visual system properties into image processing schemes is a natural approach. It offers the advantage of using

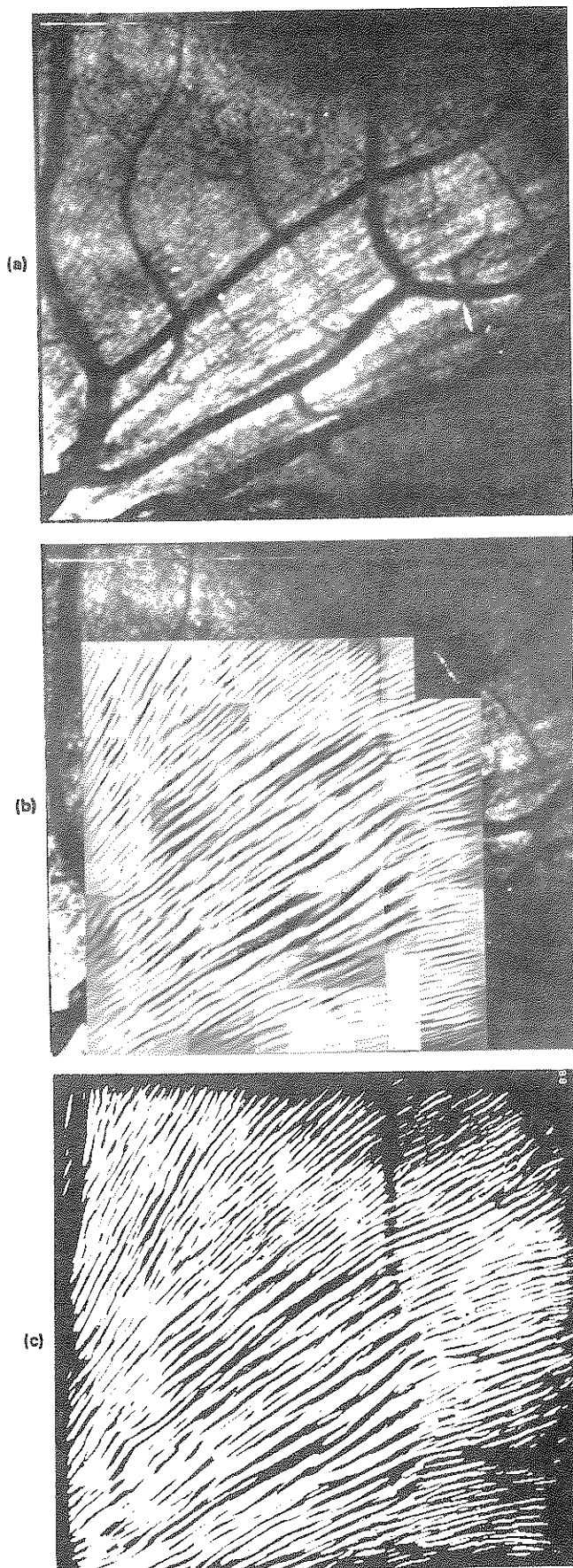


Fig. 6. Enhancement of retinal nerve fiber image. (a) Original image. (b) Image in midprocessing. (c) Fully processed image following binarization.

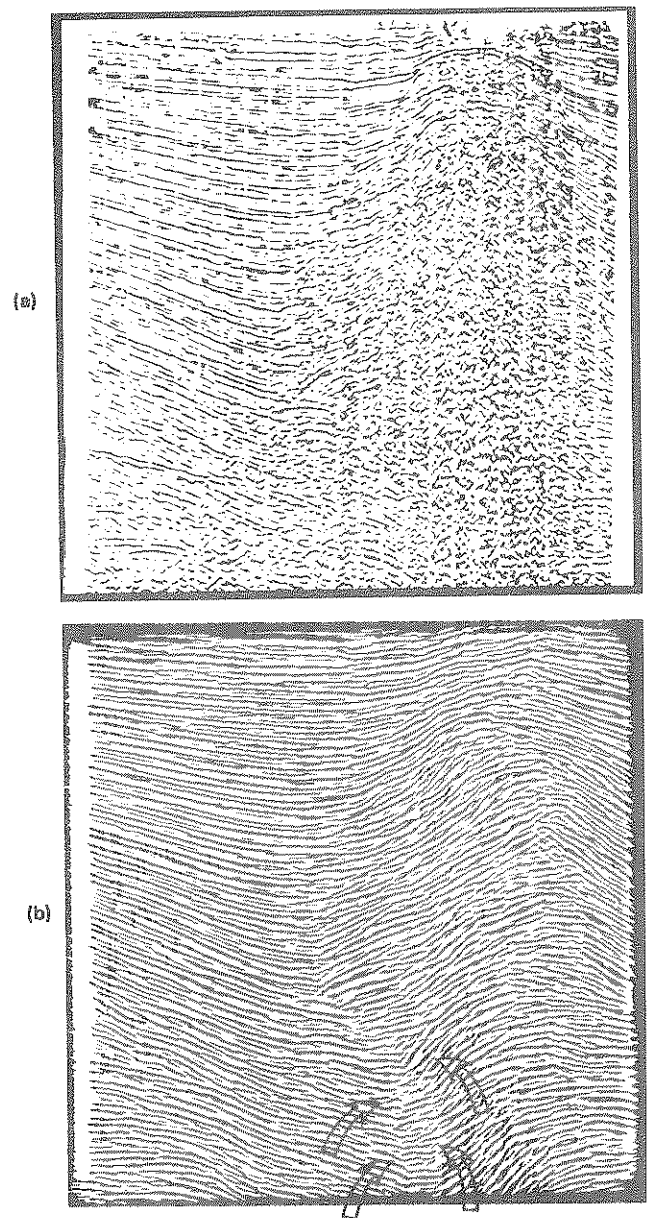


Fig. 7. Processing of seismic data. (a) Original noisy image with vertical line artifacts. (b) Processed binarized image. Note funnel-shaped area (surrounded by arrows), which is the point of interest in this image and is maintained and easier to detect in the processed image.

algorithms preferred by the best available image processing system, with results that are likely to be interpreted readily by human observers. It may also serve as a research tool for better understanding of the visual system structure and function.

Many researchers have incorporated some properties of the human visual response into the design of image enhancement and processing techniques.¹⁴⁻¹⁶ In all these applications, only the general global light intensity response of the visual system was included. Orientation-sensitive fan filters in the spatial frequency domain, based on a human visual system model, have been applied to image compression.¹⁷ The filters were applied globally to the entire image to obtain a limited set of high frequency features in different directions. A similar transform in a pyramid structure has been suggested as a

useful image processing tool.¹⁸ A fan filter was also used to remove parallel line features in various applications.^{19,20} Removing or enhancing a striated pattern using a global filter is possible only in cases in which the pattern consists of straight parallel lines. When the pattern curves and changes orientation slightly throughout the picture, a local adaptive fan filter should be applied. The common features of most adaptive image processing techniques are computation of local image measures followed by application of local measures to control adaptive processing. These local imaging measures are computed over a region defined by the processing window and can be recomputed numerous times, depending on the extent of overlapping of those windows.²¹ Such a filter was used to filter out dune lines from Landsat images,²² and a nonlinear, nondirectional filter was used to enhance fingerprint and seismic data.³

The algorithm described here combines the orientation sensitivity and band-limiting properties of the visual system's simple cells with the adaptive, spatially local nature of the receptive cells' organization. The filters were implemented explicitly with bandwidth and orientation sensitivity that match those recorded from cells. In addition, a preliminary attempt to represent the lateral parallel processing was implemented in the spiral progression of the algorithm in space, and the direction in neighboring receptive fields was used to limit the range of search for the orientation of striations. (In parallel processing, such effect would require recursive application of the process.) This additional layer of adaptation was found effective in reducing the calculation time and errors. It also highlighted the limitations of a model with only one size [Fig. 4(b)] of receptive field in processing areas of higher curvature or multiple directions, as in the case of a delta point in the fingerprint. The improvement achieved with the use of a smaller window size [Fig. 5(b)] indicates that improved performance is possible at the cost of implementing more properties of the visual system. The computation cost of such expansion may be prohibitive with serial computers, but implementation with special-purpose parallel processors should be possible with current technology.

Spatial phase characteristics of simple cells were not considered in the present study; only the magnitude of the response was considered and altered. Spatial phase, however, is of great importance, as seen in the processed seismic image [Fig. 7(b)], where the funnel structure is visible mostly because of changes in phase across the funnel's border.²² This change is maintained by processing and detected easily by the human eye. This sensitivity may be associated with the fact that recorded cortical cells have symmetric or antisymmetric spatial responses corresponding with the sine and cosine components of the Gabor function expansion. Adding such phase consideration to this model should further enhance the detection of borders between areas of different textures.

5. ACKNOWLEDGMENTS

This work was supported in part by grants R01-EY05450 and R01-EY05957 from the National Institutes of Health and a grant from the Alcoa Foundation. I thank Tami Peli and Lawrence Arend for valuable discussions and suggestions and Steven Shapiro for important programming help.

6. REFERENCES

1. E. Peli, T. R. Hedges III, and B. Schwartz, "Computerized enhancement of retinal nerve fiber layer," *Acta Ophthalmol.* 64, 113-122 (1986).

2. Y. J. M. Pouliquen, "Fine structure of the corneal stroma," *Cornea* 3, 168-177 (1985).
3. A. F. Lehar and R. A. Gonsalves, "Locally adaptive enhancement, binarization, and segmentation of images for machine vision," in *Applications of Digital Image Processing VII*, A. G. Tescher, ed., Proc. SPIE 504, 183-188 (1984).
4. G. B. Arden and J. J. Jacobson, "A simple grating test for contrast sensitivity: preliminary results indicate value in screening for glaucoma," *Invest. Ophthalmol. Vis. Sci.* 17, 23-32 (1978).
5. S. Marcelja, "Mathematical description of the responses of simple cortical cells," *J. Opt. Soc. Am.* 70, 1297-1300 (1980).
6. D. Gabor, "Theory of communication," *J. Inst. Electr. Eng.* 93, 429-457 (1946).
7. J. G. Daugman, "Uncertainty relation for resolution in space, spatial frequency, and orientation optimized by two-dimensional visual cortical filters," *J. Opt. Soc. Am.* A:2, 1160-1169 (1985).
8. R. L. DeValois, D. G. Albrecht, and L. G. Thorell, "Spatial frequency selectivity of cells in macaque visual cortex," *Vision Res.* 22, 545-559 (1982).
9. D. G. Hubel and T. N. Wiesel, "Sequence regularity and geometry of orientation columns in the monkey striate cortex," *J. Comp. Neurol.* 158, 267-293 (1974).
10. J. G. Verly and T. Peli, "Circular harmonic analysis of PSFs corresponding to separable polar-coordinate frequency responses with emphasis on fan filtering," *IEEE Trans. Acous. Speech Sig. Proc.* ASSP-33, 300-307 (1985).
11. W. R. Levick and L. N. Thibos, "Analyses of orientation bias in cat retina," *J. Physiol.* 239, 243-261 (1982).
12. J. A. Movshon, "Two-dimensional spatial frequency tuning of cat striate cortical neuron," in *Society for Neuroscience Abstracts* (9th annual meeting, Atlanta, Ga.), p. 799 (1979).
13. H. E. Olimb, T. F. Krile, and J. F. Walkup, "Optical enhancement of degraded fingerprints," *J. Opt. Soc. Am. A* (Special Edition: 1985 Annual Meeting), p. 38 (1985).
14. W. Frei, "Image enhancement by histogram hyperbolization," *Computer Graphics and Image Processing* 6, 286-294 (1977).
15. B. Chanda, B. B. Chaudhuri, and D. Dutta Magumder, "Some algorithms for image enhancement incorporating human visual response," *Pattern Recognition* 17, 423-428 (1984).
16. T. G. Stockham, Jr., "Image processing in the context of a visual model," *Proc. IEEE* 60, 828-842 (1972).
17. A. Ikonomopoulos and M. Kunt, "High compression image coding via directional filtering," *Signal Processing* 8, 179-203 (1985).
18. A. B. Watson, "The cortex transform: rapid computation of simulated neural images," *Computer Vision, Graphics, and Image Processing* (in press).
19. T. Peli and J. G. Verly, "Digital line-artifact removal," *Opt. Eng.* 22(4), 479-484 (1983).
20. J. G. Moik, "Image restoration," in *Digital Processing of Remotely Sensed Images*, pp. 77-126, NASA, Washington, D.C. (1980).
21. V. T. Tom, "Adaptive filter techniques for digital image enhancement," in *Digital Image Processing: Critical Review of Technology*, A. G. Tescher, ed., Proc. SPIE 528, 29-42 (1985).
22. M. R. Turner, "Texture discrimination by Gabor functions," *Biol. Cybern.* 55, 71-82 (1986).



Eli Peli was born in Tel Aviv, Israel, in 1951. He received B.Sc., cum laude, and M.Sc. degrees in electrical engineering from the Technion—Israel Institute of Technology in 1976 and 1979, respectively, and a doctorate degree in optometry from the New England College of Optometry in 1983. He is assistant professor of ophthalmology at Tufts University School of Medicine, assistant scientist at the Eye Research Institute, associate in ophthalmology at Harvard Medical

School, and director of the Low Vision Service at New England Medical Center, Boston. His principal research interests are image processing in relation to visual function and clinical psychophysics. He also maintains an interest in control of eye movements and binocular vision. He is a fellow of the American Academy of Optometry and a member of the Association for Research in Vision and Ophthalmology and SPIE.